Journal of Sol-Gel Science and Technology, 3, 189–197 (1994)

Polymetalates Based Organic-Inorganic Nanocomposites

P. JUDEINSTEIN[1] AND H. SCHMIDT

Institut für Neue Materialen, Universität des Saarlandes, Geb. 43, D-66123 Saarbrücken, Germany

Abstract. New nanocomposites materials have been synthesized. They present electrochemical and photochromic properties. They are based on a hybrid organic-inorganic network, in which tungsten heteropolyoxometalates ($PW_{12}O_{40}^{3-}$, $SiW_{12}O_{40}^{4-}$, $W_{10}O_{32}^{4-}$, polymeric tungstate) are entrapped. High tungsten ratios could be reached and films or bulk materials have been obtained. The structure of these materials is described on the basis of multi-spectroscopic investigations (IR, EPR, NMR). Electrochemical redox reactions have been observed in thin films. Dark blue reversible coloration of the materials is obtained under UV irradiation. The photochromic mechanism has been investigated and shows the reversible formation of carbonyl group.

Keywords: nanocomposites, sol-gel, heteropolymetalates, photochromics, electrochemical properties

1 Introduction

Nanotechnologies are looking to reach high densities of data storage. Electrochromic or photochromic properties of some materials could be used for this purpose. Using materials with sensitive units as small as possible, and with the highest contrast variation between both states is the key to increase data storage. Entrappement of electro or photo-responsive molecular units into a polymeric or glassy matrix could perform these goals [1]. Such high-tech substances are described as nanocomposites [2]. It is emphasized that they can combine and synergize the properties of the solid matrix, and the incorporated molecules or clusters.

The sol-gel process is an interesting alternative route to prepare such kind of materials. The low temperature process involved allows the synthesis of materials which could not be prepared by conventional methods [3]. Moreover, the control of the viscosity of the mother solution can lead to prepare films of variable thicknesses on different surfaces, and monoliths of various shapes [4].

[1]Present address: Laboratoire de Chimie Structurale Organique (CNRS URA 1384), Université Paris-Sud, Bât 410, 91405 Orsay, France.

This paper presents the synthesis, the characterization and some aspects of the electrochemical and photochromic properties of some organic-inorganic nanocomposites.

The active starting materials are tungsten heteropolyoxometalates (or POM) ($PW_{12}O_{40}^{3-}$, $SiW_{12}O_{40}^{4-}$, $W_{10}O_{32}^{4-}$, polymeric tungstate). These polyanions have been extensively studied [5]. They present interesting properties as high solubility in many solvents depending on the counter-ion, a quite small size (around 10 Å in diameter) and a very high electronic density. The presence of many highly oxidized metallic centers make polyoxometalates good candidate for many applications [6] (catalysts, electron microscope tracers, analytical reagents, materials for photochemistry and electrochromism). Many studies are dealing with their stabilization by entrapment in polymeric networks as cross-linking reagents [7], into a silica based glass structure [8] or clays [9], or their chemical anchoring to an organic backbone [10].

In this study, an organic-inorganic network based on silica clusters and polyether chains is chosen as a matrix [11]. Very high concentration of the POM species can be obtained from the high solvating behavior of polyether chains, containing lone pair electrons on oxygen atoms [12].

Solid and transparent materials are obtained tailoring the size, structure and distribution of silica clusters. The properties of these materials in regard to their structure are described.

2 Experimental

All chemical reagents are commercially available and are used as purchased (Fluka, Aldrich), these included: tetraethoxysilane (TEOS), tetraethyleneglycol (TEG), silicotungstic and phosphotungstic acids (respectively H_4SiW_{12} and H_3PW_{12}), sodium tungstate (Na_2WO_4) and hydrochloric acid. J.P. Launay (Université de Toulouse) is gratefully thanked for the gift of a pure sample of potassium decatungstate ($K_4W_{10}O_{32}$). Deionized water was used in all experiments.

Infrared spectra were obtained with an IFS25 Bruker Fourier Transform spectrometer. The probes were thin films deposited on two-side polished silicon wafers. Spectra were recorded in the range 4000–400 cm^{-1} with 2 cm^{-1} resolution.

NMR experiments have been performed with AC 200 Bruker and AM 200 Bruker spectrometers, respectively for liquid and solid state experiments, following standard procedures (proton broad band decoupling ($\{^1H\}-^nX$) for liquid NMR measurements, magic-angle spinning (4 kHz) and cross-polarization for solid state NMR (CP-MAS).

Photochromic reactions have been conducted with a 750 W Xenon lamp lighting. Optical absorption measurements were made with an Omega 10 spectrometer (Bruins Instruments) with 2 nm optical resolution.

Electrochemical measurements have been performed with an EGG potentiostat (model Versaterm™). A classical three electrode cell has been used for these experiments. The working electrode was a thin film of material deposited on transparent electronic conductor substrate (glass/ITO). Area of the electrode was about 1 cm^2. The electrolyte was a 1M solution of $LiClO_4$ in propylene carbonate. Potentials are measured in respect to an Ag/Ag^+ reference electrode.

3 Synthesis and Characterization

3.1 Gel Preparation

For the sake of clarity, the synthesis of two representative materials is described.

Type I gel demonstrates that a mixture of TEOS and TEG could be used to solve high ratios of POM. After that, chemical species leading to the matrix evolve to give a more and more viscous solution, and thereafter a bulky transparent material.

In type II, the POM species are formed in situ by acidification of Na_2WO_4 in the TEOS/TEG solution. Viscosity of solution evolves leading to a transparent gel.

All reactions are performed without additional solvents. As a consequence less evaporation leading to a less shrinkage proceed during the drying of films or bulk. More homogeneous films or less cracked bodies can be obtained in that way.

Type 1. 2.08 g of TEOS (10^{-2} mole) were added to 1.94 g of TEG (10^{-2} mole) and 0.45 g of water (2.5×10^{-2} mole), under vigorous stirring. The mixture was heated to 60°C and stirred 10 minutes. Then 1.98 g of POM (6.6×10^{-4} mole) ($H_4SiW_{12}O_{40}$ or $H_3PW_{12}O_{40}$) was added, and the blend was mixed up to the total dissolution of POM. Then, thin films could be prepared by spin or dip-coating and placed in an oven 70°C for 48 hours. Transparent monoliths could be also obtained in a few days. Transparent materials could be also prepared with different quantities of TEG (0.005 to 0.015 mole) or different molecular weight polyethylene glycol (MW: 100 to 600) and varying POM ratios (2×10^{-5} to 6.6×10^{-4} mole). Nonetheless, initial viscosity and gelling time are strongly dependent from these ratios.

Type 2. 2.08 g of TEOS (10^{-2} mole) are added to 1.94 g of TEG (10^{-2} mole) and vigorously stirred. Then, a solution containing 0.165 g of Na_2WO_4 (5×10^{-4} mole) dissolved in 0.9 g of water (5×10^{-2}) is added. Then, 120 μl of concentrated chlorohydric acid (1.5×10^{-3} mole)

are droply added under vigorous stirring. Thin films or bulk could be obtained by the same way as for type 1 compounds. Various amounts of Na_2WO_4 or HCl have been used, and the influence of the acidity ratio Z ($Z = [H^+]/[W]$) has been studied. Transparent photochromic materials are obtained in a few days (RT) for $Z \geq 1$, while a white gelatinous precipitate is obtained in a few minutes for $Z < 0.7$. In the former conditions ($Z \geq 1$), the pH of the solution is acidic and polymeric silica network should develop. A basic pH of the solution has been measured in the latter conditions ($Z < 0.7$), and the formation of a dense silica network is expected [14].

In order to increase the stability of the different layers and the bulk, all materials have been heat treated at least 90°C during 48 hours. No changes of properties have been observed with further treatments.

Thereafter, the ratio W/Si represents the number of W atoms per TEOS molecule.

3.2 *Gel Characterization*

Organic-Inorganic Network

IR. Broad bands centered around 1170 cm^{-1} (ν_{C-O-C}) and 1070 cm^{-1} (ν_{Si-O-C}, $\nu_{Si-O-Si}$) indicates the development of a network during the gel formation. However, their broadness and overlapping with sharp and intense vibrations of the POM species prohibit further investigations. Organic groups are also evidenced by signals around 2940–2880 cm^{-1} (ν_{C-H}). Hydration of the film is evidenced by two bands around 3500 and 1600 cm^{-1}.

NMR. ^{13}C and ^{29}Si NMR experiments have been performed for materials synthesized with various amount of POM. For the whole composition range, ^{13}C NMR evidences that all the ethoxy groups have been removed from the TEOS. Some bonds between silicon atoms and TEG molecules ($\cdots Si-O-CH_2CH_2O- \cdots$) are measured (5–10%). The important ratio of non-bonded TEG molecules leads to the high mobility of the whole TEG phase on the NMR timescale. Figure 1 presents the ^{29}Si CP-MAS NMR of samples obtained with different ratios of SiW_{12}. They present three broad peaks around $-93, -102$ and -110 ppm, characteristic of Q^2, Q^3 and Q^4 Si coordination shells. A narrow peak is also observed at -85 ppm, representative of the silicon atom of the $H_4SiW_{12}O_{40}$ cluster. This points out the preservation of the Keggin entity in the final compounds. The slight broadening for this signal in the solid state indicates a moderate lowering of the mobility of the clusters with the gelation. Probing the respective intensity of the three broad signals of silica clusters with POM concentration leads only to tiny changes. The same conclusion could be drawn if POM catalysis was changed for HCl catalysis ($0.005 < H^+/Si < 0.133$). Then, it appears that the formation of silica clusters, and their morphology is poorly affected by severe changes in the catalysis media and ratios. Liquid state NMR has been performed on such systems (Fig. 1d). The definitive shape of the spectra, with Q^2 and Q^3 signals is observed just after mixing of reactants. The presence of silicon in the probe enables the observation of Q^4 species. Only slight changes of the spectra could be observed up to the gel point. It appears the formation of the silica clusters was found extremely quick, in regard to the gelation time.

This two points reflect some strong differences with pure silica systems. In these systems the SiO_2 network evolves still a long time after the gel point [15], and a slight change of pH or concentration could induce radical changes in the silica structure [16]. Previous studies of such organic-inorganic systems evidence the very bushy structure of silica particles and a low compatibility between the organic (TEG) and inorganic (SiO_2) phases [13]. The high viscosity of the TEG reduces the mobility of molecules and oligomers, and most of the inorganic network should develop at the beginning of the process.

POM Species

IR. IR spectra of materials with higher POM concentrations show sharp and intense peaks corresponding to POM species (vide infra).

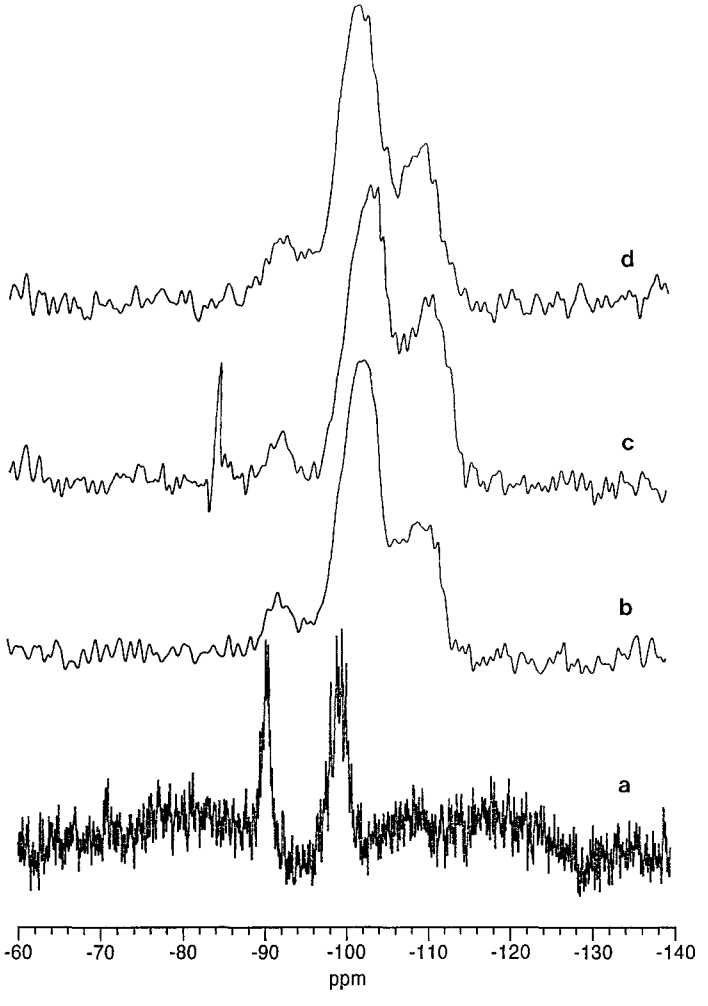

Fig. 1. ^{29}Si NMR of TEOS/TEG/x system (from bottom to top) a) liquid state, after mixing of chemical, x = SiW_{12}, W/Si = 0.1. b) CP-MAS, x = SiW_{12}, W/Si = 0.1. c) CP-MAS, x = SiW_{12}, W/Si = 0.8. d) CP-MAS, x = HCl, $[H^+]/[TEOS]$ = 0.01.

The bands wavenumbers are rather similar to those observed for POM in solution in common solvents [17]. The small shifts observed therein reflect the anion-cation and anion-solvent interactions.

ESR. ESR is an efficient and sensitive spectroscopy to characterize polymetalates. Samples have been reduced under a low power UV light before investigation. Measurements have been performed at 90 K. Spectra are presented on Figure 2.

Type 1 materials present isotropic signal centered at g = 1.816 for $H_3PW_{12}O_{40}$ systems, and a rather orthorhombic signal for $H_4SiW_{12}O_{40}$ based materials (g_x = 1.855, g_y = 1.823, g_z = 1.782). These values are in perfect agreement with values reported in the literature (18). The orthorhombic symmetry of $H_4SiW_{12}O_{40}$ is explained by electronic localization at a temperatures around 90 K.

ESR spectra obtained with **type 2** gels, and different Z ratios are also presented on Figure 2. All spectra have rather complex structures and could be only interpreted as a mixture of various tungstic species. Lower Z ratios lead to a two signal system. One is looking as a distorted axial site, with g = 1.849 and about 40 G wide and the same spectrum has been obtained with $K_4W_{10}O_{32}$ doped TEOS/TEG structures. These

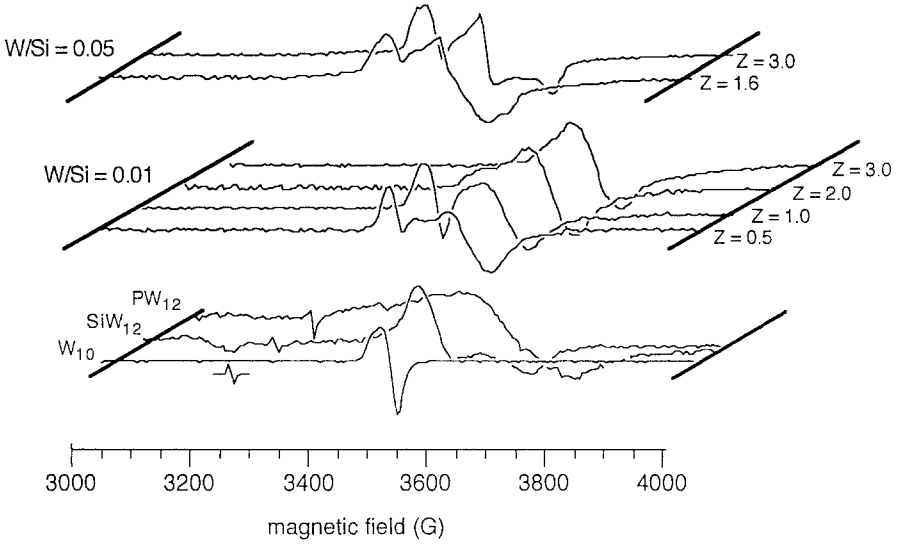

Fig. 2. EPR of POMs based nanocomposites. bottom: doped with defined heteropolymetalate middle and top: obtained with various W/Si and Z ratios.

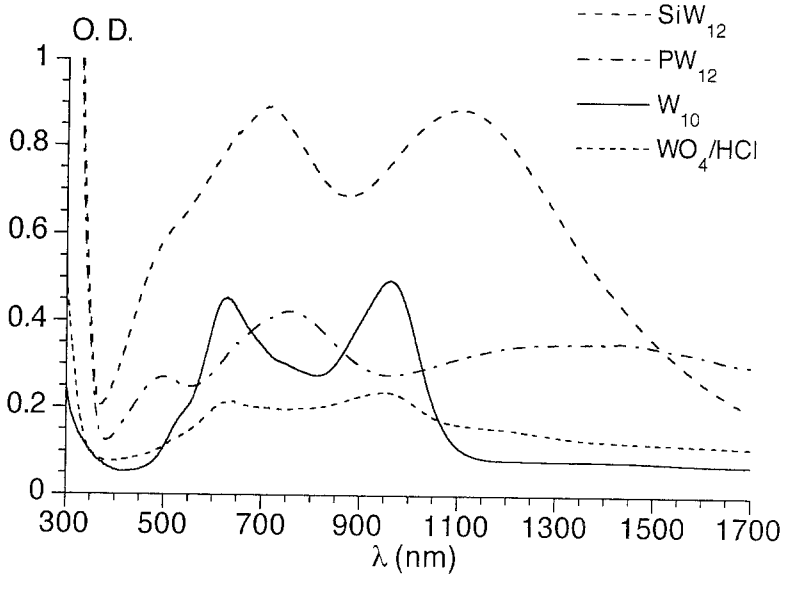

Fig. 3. UV-vis absorption of POMs base nanocomposites.

values are in good agreement with the study of reduced decatungstate species dissolved in various solvents [19]. The other signal is rather broad (100 G) and centered around $g = 1.75$. Such a low g value reflects the presence of polymeric tungstate species. Higher Z ratios materials are characterized by the increase of the second component, and the apparition of a new orthorhombic-like signal with g values of 1.85, 1.80, 1.75. Such a signal is rather similar to those observed for Keggin polymetalates solutions [18] [20]. It is well established that mixing Na_2WO_4 and TEOS in acidic water leads to silicotungstate. The low pH of the mixture could be compatible with the formation of $SiW_{12}O_{40}^{4-}$ [18].

The presence of polymetalates species in these materials especially $W_{10}O_{32}^{4-}$ is confirmed by visible spectrometry. Figure 3 presents the op-

tical absorption spectra of organic-inorganic thin films composites doped with $H_3PW_{12}O_{40}$, $H_4SiW_{12}O_{40}$, $K_4W_{10}O_{32}$ and Na_2WO_4/HCl. These spectra present some defined band and are characteristic of reduced POM molecular species, associated with electron hopping process. $H_3PW_{12}O_{40}$ and $H_4SiW_{12}O_{40}$ doped materials present the familiar shape of Keggin species with maxima around 500, 745 and 1270 nm for $H_3PW_{12}O_{40}$ (490, 718, 1108 nm for $H_4SiW_{12}O_{40}$ containing films) [21]. Spectra of $K_4W_{10}O_{32}$ and Na_2WO_4/HCl doped materials are quite comparable with two maximum at 627 and 959 nm. Their shape is close to the two electron reduced $W_{10}O_{32}^{4-}$ clusters in aqueous solution.

The structural investigation of these materials demonstrate their nanocomposite features. Small tungsten oxide clusters are entrapped in an organic-inorganic matrix.

The matrix is based on organic and inorganic domains, more or less connected together. Small particles of silica are formed from hydrolysis-condensation of TEOS. However, their size, morphologies and distribution do not preclude to the transparency of the bulk and films. The rigid backbone of this material is based on silica, as suitable organic chains help the dissolution of high quantities of POM. The moderate grafting of both phases increases the rheological properties of the sol leading to great filmability. Figure 4 presents an idealized view of POM species entrapped in a TEOS/TEG matrix. The length of the TEG chains has the same magnitude as POM clusters. Then a few groups linked to TEOS molecules could form an efficient network to entrap these molecules.

The strong chemical similarity of PEG and water explain the high solubility POM species in such organic-inorganic matrices. The active clusters of POM are homogeneously distributed in the materials, and their individual properties remains in the film, as observed from EPR and visible measurements. Such tungsten-oxide clusters could be introduced as raw materials or obtained in situ by acidification of sodium tungstate. This interesting route leads to different species, depending Z and the tungsten concentration [5] [22]. Decatungstate is the major species for moderate acid ratio ($Z < 2$) while

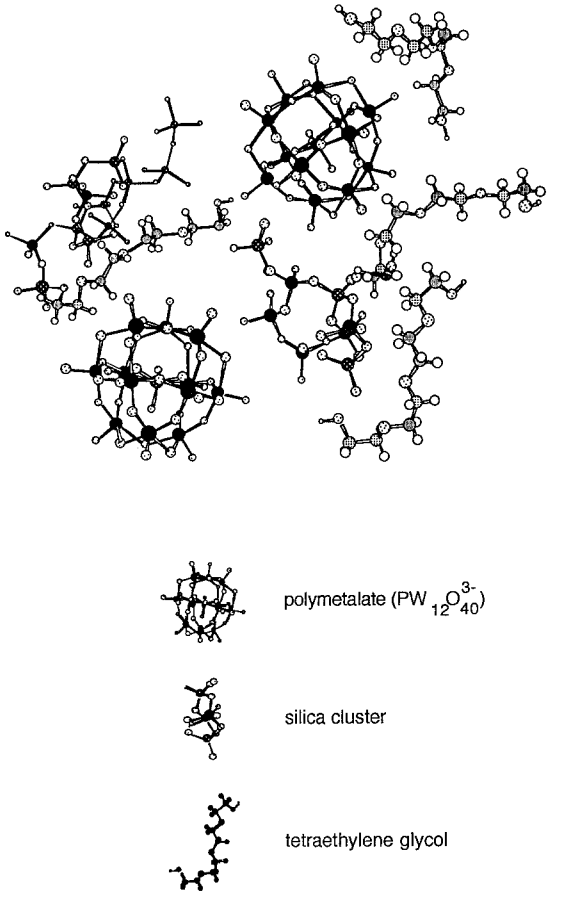

Fig. 4. Idealized structure of POMs based nanocomposites.

polymeric tungstate or Keggin species are observed for higher ratios. These results address the complex equilibrium found in the tungsten aqueous chemistry. The same kind of diagram of predominance has been described [20]. In water, the presence of decatungstate is measured for pH around 5 ($Z > 1.5$), more condensed metatungstic species (Keggin like) for pH < 5, while polymeric tungstate or tungsten oxide gels are formed for pH around 1 ($Z > 2$).

4 Properties

4.1 Optical Properties

The optical absorption of the different systems is related to the exposure time up to a saturation level. Bleaching occurs in contact with oxygen,

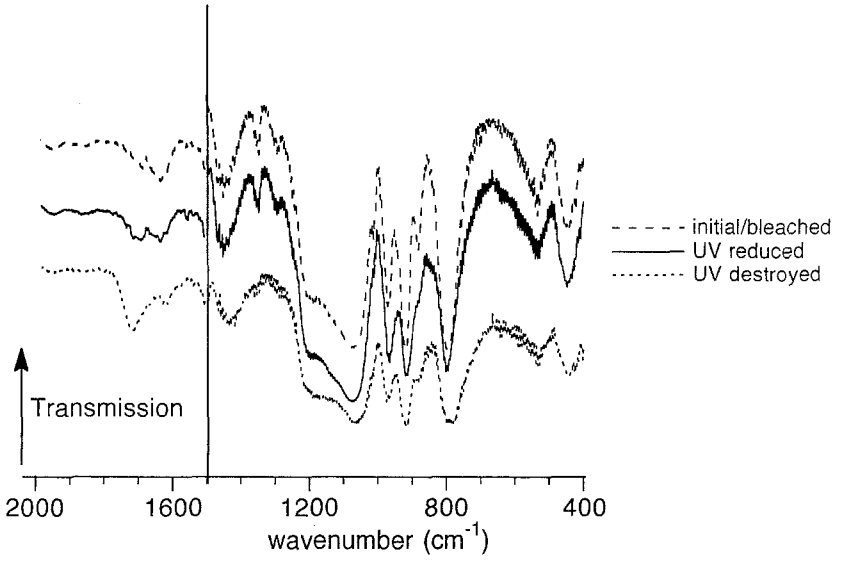

Fig. 5. IR monitoring of coloring, bleaching and degradation process in SiW_{12} based materials.

with typical time of about 2 hours for lower W concentrations, and up to 48 hours for higher W ratios and deep coloration level. No bleaching has been observed when the layer or the bulk is protected from the oxygen contact, even after 3 months. The photochromic cycling behavior of such films [blue, bleach,...] is quite reversible for tenths of cycles if a moderate irradiation power is used (3/4 of saturation level). An irreversible degradation has been observed for long illumination time.

Figure 5 presents the monitoring of the mechanism of the photochromic reduction and the degradation process by infrared spectroscopy. Initially, the film presents the set of vibrations of $H_4SiW_{12}O_{40}$ polymetalates in the range 1020 cm^{-1}–700 cm^{-1} (e.g. 1014 cm^{-1} [ν_{asSi-O}], 971 cm^{-1} [$\nu_{asW=O}$], 921 cm^{-1} [$\nu_{asSi-O/W-O-W}$], 884 cm^{-1} [$\nu_{asW-O-W}$], 798 cm^{-1} [$\nu_{asW-O-W}$]) [17], the vibration bands of the matrix in the range 1020 cm^{-1}–1400 cm^{-1} and a band around 1600 cm^{-1} characteristic of the hydratation water. After a moderate light exposure, characteristic changes of the spectrum are observed. The intensity of the set of bands relative to the POM is strongly decreasing, a broadening and a slight shift of these bands is measured. Simultaneously, a new band around 1710 cm^{-1} is also observed, corresponding to the formation of carbonyl bonds ($\nu_{C=O}$). This corresponds to the oxidation product of TEG molecules. All these changes are strictly reversible under oxygen reoxidation. Nevertheless, if the UV light exposure time is too long, the properties of the films degrade, and the intensity of the vibration corresponding to carbonyl groups increases drastically. Afterwards, this band does not change, even after a few weeks. Irreversible variation of the bands corresponding to the matrix structure at 1320 cm^{-1} and 1450 cm^{-1} is also observed. Same effects are observed for lower POM contents.

All these observations could be related to the photochromic mechanism involved in such materials. It clearly evidences the reduction of the POM and the simultaneous oxidation of the TEG molecules. Both reactions are reversible up to a saturation level where the material is irreversibly destroyed. The structure of the POM molecule is affected by the photochemical reduction. This phenomenon has been observed during the reduction of POM in solution [23], and described as a slight structural modification of their structure, mainly changes of the bond lengths and angles [24]. The reduction process of the POM corresponds to the simultaneous oxidation of the matrix. For low POM reduction ratios, the reversible formation of a few carbonyl group is observed as described in alcoholic solutions [21]. They are probably the result of oxi-

dation of the end OH group of TEG molecules, thus leading to aldehydes RCHO. The following mechanism could be suggested (R is the radical of the PEG chain):

$$POM^{n-} \xrightarrow{h\nu} POM^{*n-}$$

$$POM^{*n-} \xrightarrow{k_{-1}} POM^{n-}$$

$$POM^{*n-} + RCH_2OH \longrightarrow POM^{(n+1)-} + R\dot{C}HOH + H^+$$

$$POM^{n-} + R\dot{C}HOH \longrightarrow POM^{(n+1)-} + RCHO + H^+$$

These reactions are quite reversible, leading back to the OH function. For deeper reduction ratios, more carbonyl groups are formed, and the reaction could also extend to the synthesis of carboxylic acid functions RCOOH. Then, the possibility to break and oxidize some ether links should be considered. This step leads to smaller organic molecules and is also fully irreversible. No formation of C–C double bonds could be suggested, as it was observed previously for some $H_3PW_{12}O_{40}$/poly(vinylalcohol) materials [25].

4.2 *Electrochemical Properties*

Figure 6 presents the voltamograms of TEG/TEOS based materials doped with $H_3PW_{12}O_{40}$ and $H_4SiW_{12}O_{40}$ species. Well defined signals could be observed for reduction and oxidation processes.

Thin films of $H_3PW_{12}O_{40}$/TEOS/TEG materials (with W/Si = 0.1) present one set of peaks, $E_{red} = -880$ mV; $E_{ox} = -810$ mV ($\Delta E = 70$ mV). The relationship between intensity and scan rates does not follow any usual behavior encountered for diffusion limited processes or species firmly grafted to a surface [26]. A good stability of this electrochemical reaction is observed. After 500 cycles, and more than one week in the electrolyte no changes are detected. The quantity of charge injected in POM, measured as the area of the peak, remains constant with the scanning rate (10 μC/cm^2). An increase of tungsten concentration to W/Si = 0.8 leads to an increase of the injected charge up to 130 μC/cm^2. $H_4SiW_{12}O_{40}$/TEOS/TEG presents three redox reactions ($E_{red1} = -360$ mV, $\Delta E_1 = 200$ mV; $E_{red2} = -610$ mV, $\Delta E_2 = 240$ mV, $E_{red3} = -870$ mV, $\Delta E_3 = 380$ mV for $v = 50$ mV/s).

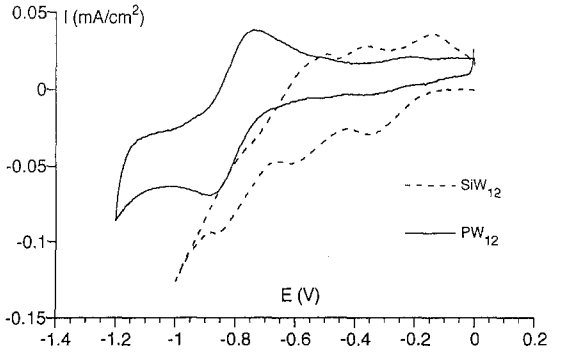

Fig. 6. Cyclic voltamogramm of nanocomposite electrode doped with SiW_{12} and PW_{12}.

These electrodes are quite stable in PC/$LiClO_4$ electrolytes, and injected charges for W/Si = 0.1 is about 10 μC/cm^2 while about 100 μC/cm^2 for W/Si = 0.8.

These results point out the possibility to use nanocomposites for electrochemical purposes. The flexibility of the involved chemistry leads to the tailoring of the materials. In the TEOS/TEG matrix, the system seems to be really stable and reversible. The POM is entrapped in the matrix, and interactions with the polyether chains are strong enough to get a stable system. Such interactions are evidenced by small shifts of the redox potential, compared with POM solutions [27]. Nevertheless, the charge injected in this materials is really low, and slightly dependent on the thickness of the film. A calculation based on the assumption of the homogeneity of the materials proves that for W/Si = 0.1, only the first layer of POM in contact with the conductor is electrochemically active. In more concentrated POM systems (W/Si = 0.8), a few layers are concerned by the electron hopping. Such low yield of the electron transfer reaction is related to the very low diffusion coefficient of POM species, as determined by Forced Rayleigh Scattering ($D_{elec} \approx 10^{-12}/10^{-13}$ cm^2 s^{-1}). This means a very low mobility of the POM species in the materials [28], which explains the low frequency for POM-electrode contacts. Large ΔE values observed, and their strong dependance with the scanning rate reflects these kinetic problems, expecting a "slowly reversible" electrochemical system.

5 Conclusion

The versatility of the sol-gel process is exploited to produce new promising nanocomposites with attractive electrochemical and photochromic properties. This paper addresses a description of the structure and the properties of such hybrid materials. A good compatibility between the three components (silica, POM and TEG) leads to materials with good optical properties. The redox mechanism leading to a strong blue coloration is detailed. It evidences that reduction of the POM and oxidation of the matrix occurs simultaneously. These reactions are reversible if the redox ratio is not too high. The fine tuning of the final physical properties is obtained by the choice of the POM species entrapped in the network. The degree of freedom to create such multicomponents systems is quite infinite, leading to an innovative field for the materials chemist.

Acknowledgments

This work was supported by the Minister of Research and Culture of the State of Saarland. P.J. gratefully acknowledges support of this work by Alexander Von Humboldt-Stiftung. We are grateful to T. Reinert and D. Hoebbel for the MAS experiments results, H. Krug and P.W. Oliveira for helpful discussions.

References

1. S. Sakka and T. Yoko, Chemistry, *Spectroscopy and Applications of Sol-Gel Glasses* (Springer-Verlag, 1992), 89.
2. G. Ozin, *Adv. Mater.* **4**, 612 (1992).
3. H.K. Schmidt, Mat. Res. Symp. Proc. **180**, 961, (1990).
4. In *Sol-Gel Technology for Thin Films, Fibers, Preforms, Electronics and Specialty Shapes* (Eds. L.C. Klein, Noyes, 1988).
5. a) P. Souchay, *Ions minéraux condensés* (Masson, Paris, 1969). b) M.T. Pope, *Heteropoly and Isopolyoxometalates* (Springer-Verlag, Berlin, 1983).
6. M.T. Pope and A. Müller, Angew. Chem. Int. Ed. Engl. **30**, 34 (1991).
7. a) K. Nomiya, H. Murasaki, and M. Miwa, Polyhedron **5**, 1031 (1986). b) B. Keita and L. Nadjo, Mat. Chem. Phys. **22**, 77 (1989). c) G. Bidan and M. Lapowski, Synth. Met. **28**, C113 (1989).
8. a) K. Moller, T. Bein, and C.J. Brinker, Mat. Res. Soc. Symp. Proc. **180**, 595 (1992). b) A. Chemseddine, J. Non-Cryst. Solids **147–148**, accepted (1992).
9. a) T. Kwon and T.J. Pinnavaia, Chem. Mater. **1**, 381 (1989). b) J. Wang, Y. Tian, R-C. Wang, and A. Clearfield, Chem. Mater. **4**, 1276 (1992).
10. P. Judeinstein, Chem. Mater. **4**, 4 (1992).
11. H. Schmidt, *Spectroscopy and Applications of Sol-Gel Glasses* (Springer-Verlag, 1992), 119.
12. M. Armand, Adv. Mater. **2**, 278 (1990).
13. P. Judeinstein, J. Titman, M. Stamm, and H. Schmidt, Chem. Mater, **6**, 127 (1994).
14. R.K. Iler, *The Chemistry of Silica*, Wiley, New York, 1979.
15. F. Devreux, J.P. Boilot, F. Chaput, and A. Lecomte, Phys. Rev. A **41**, 6901 (1990).
16. L.W. Kelts and N.J. Armstrong, J. Mater. Res. **4**, 423 (1989).
17. M. Fournier, R. Thouvenot, and C. Rocchiccioli-Deltcheff, J. Chem. Soc. Faraday Trans. **87**, 349 (1991).
18. a) M.T. Pope, *Heteropoly Blues, Nato Summer School Proceedings* (Oxford 1979). b) C. Sanchez, J. Livage, J.P. Launay, and M. Fournier, J. Amer. Chem. Soc. **105**, 6817 (1983).
19. A. Chemseddine, C. Sanchez, J. Livage, J.P. Launay, and M. Fournier, Inorg. Chem. **23**, 2609 (1984).
20. A. Chemseddine, M. Henry, and J. Livage, Revue Chimie Minérale **21**, 487 (1984).
21. E. Papaconstantinou, Chem. Soc. Rev. **18**, 1 (1989).
22. M. Henry, J.P. Jolivet, and J. Livage, *Chemistry, Spectroscopy and Applications of Sol-Gel Glasses* (Springer-Verlag, Berlin, 1992) 117.
23. K. Eguchi, Y. Toyozawa, N. Yamazoe, and T. Seyama, J. Cat. **83**, 32 (1983).
24. a) Y. Jeannin, J.P. Launay, and M.A. Seid Sedjadi, Inorg. Chem. **19**, 2933 (1980). b) N. Casân-Pastor, P. Gomez-Romero, G.B. Jameson, and L.C.W. Baker, J. Am. Chem. Soc. **113**, 5658 (1991).
25. J.C. Carls, P. Argitis, and A. Heller, J. Electrochem. Soc. **139**, 786 (1992).
26. N.A. Surridge, J.C. Jernigan, E.F. Dalton, R.P. Buck, M. Watanabe, H. Zhang, M. Pinkerton, T.T. Wooster, M.L. Longmire, J.S. Facci, and R.W. Murray, Faraday Discuss. Chem. Soc. **88**, 1 (1989).
27. B. Keita, D. Bouaziz, and L. Nadjo, J. Electrochem. Soc. **135**, 1 (1988).
28. P. Judeinstein, P.W. Oliveira, H. Krug, and H. Schmidt, Chem. Phys. Lett., **220**, 35 (1994).